



PII: S0895-9811(97)00017-5

Geochemistry of the Estrela Granite Complex, Carajás region, Brazil: an example of an Archaean A-type granitoid

CARLOS EDUARDO DE MESQUITA BARROS^{1,2,3,4}, ROBERT DALL'AGNOL⁴, PIERRE BARBEY^{2,3} and ANNE-MARIE BOULLIER²

1 CNPq, Brasília, Brazil.

2 CRPG-CNRS (UPR-9046), B.P. 20, 54501 Vandoeuvre Cedex, France

3 Université Henri Poincaré (JE-249) Vandoeuvre, France

4 Dept°. Geoquímica e Petrologia — Grupo Petrologia de Granitos — Universidade Federal do Pará, Belém, Brazil

(Received June 1995; accepted November 1996)

Abstract — The Estrela Granite Complex is an Archaean granite batholith which outcrops to the east of the Serra dos Carajás, northern Brazil. This complex, surrounded by supracrustal sequences metamorphosed under medium- to high-grade conditions, was affected by heterogeneous ductile deformation. Petrographically, this body exhibits a relatively wide facies variation where hornblende±pyroxene monzogranites and hornblende±biotite monzogranites dominate. The high alkali contents, the extremely high $FeO/(FeO+MgO)$ ratios and the elevated values of some high field strength elements (HFSE) demonstrate the alkaline affinities of the studied rocks. Al_2O_3 -poor metaluminous monzogranites and Al_2O_3 -rich weakly peraluminous monzogranites have been distinguished. Partial melting of meta-igneous or undepleted granulitic rocks could generate such granitic magmas. On the basis of its geochemical signature, the Estrela Granite Complex is thought to be an unequivocal example of A-type granite magmatism, being thus very different from granitoids reported southward in the Rio Maria Archaean granite-greenstone terrain, where the calc-alkaline and trondhjemitic suites are predominant. © 1997 Elsevier Science Ltd

Resumo — O Complexo Granítico Estrela é um corpo granítico de idade arqueana que aflora a leste da Serra dos Carajás, região norte do Brasil. Este batólito corta uma seqüência de rochas supracrustais metamorfasadas em condições de médio a alto grau. O Complexo Granítico Estrela foi afetado por deformação dúctil de modo heterogêneo. Ele apresenta uma ampla variação faciológica, porém, predominam hornblenda±piroxênio monzogranitos e biotita±hornblenda monzogranitos. Os altos valores de álcalis, as razões $FeO/(FeO+MgO)$ extremamente elevadas e os altos teores de Zr, Nb e Y evidenciam a sua afinidade com rochas de assinatura alcalina. Dois grupos de rochas foram distinguidos: um relativamente enriquecido em Al_2O_3 (fracamente peraluminoso) e o outro relativamente empobrecido em Al_2O_3 (metaluminoso). A fusão parcial de rochas meta-ígneas ou rochas granulíticas não depletadas poderia explicar a origem dos magmas graníticos em consideração. A assinatura geoquímica do Complexo Granítico Estrela permite compará-lo aos granitos do tipo A, contrastando fortemente com as rochas granitóides da região de Rio Maria, onde predominam séries cálcio-alcalinas e trondhjemiticas.

INTRODUCTION

Geochronological studies have defined the Archaean age for the Carajás Mining Province (Hirata *et al.*, 1982; DOCEGEO, 1988), including both the Serra dos Carajás region and the Rio Maria granite-greenstone terrain (Wirth *et al.*, 1986; Machado *et al.*, 1991; Macambira, 1992; Macambira and Lafon, 1994). Petrographic, geochemical and structural features of some Archaean granitoids, outcropping in the above areas, have also been investigated in recent years (Medeiros and Dall'Agnol, 1988; Lindenmayer, 1990; Jorge João *et al.*, 1991; Duarte, 1992; Souza, 1994; Althoff *et al.*, 1994). Most of the studied complexes are located in the Rio Maria region (100 km south from the Carajás Mining Province), where the granitoids exhibit dominantly tonalitic-to-trondhjemitic or granodioritic compositions (e.g., Arco Verde Tonalite, Mogno Trondhjemitic, Rio Maria Granodiorite; Althoff *et al.*, 1994; Huhn *et al.*, 1988; Medeiros, 1987; respectively), although monzogranites also occur (Mata Surrão, Xinguara and Guarantã granites; Duarte, 1992; Leite and Dall'Agnol, 1994; Althoff *et al.*, 1994; respectively). The U-Pb zircon ages of those granitoids range from 2.96 Ga to 2.87 Ga (Macambira, 1992; Macambira and Lafon, 1994).

The available geochronological data of the Archaean gneissic and granitoid complexes in the Serra dos Carajás region, located in the northern part of the province, are still limited in number. Lindenmayer (1990) described in the Salobo area trondhjemitic gneisses belonging to the Xingu Complex and the Old Salobo Granite, whose U-Pb zircon ages are 2851 ± 4 Ma and 2573 ± 2 Ma, respectively (Machado *et al.*, 1991). Ferreira and Serfaty (1988) and Jorge João *et al.* (1991) have also presented preliminary geochemical data on the Estrela Granite Complex.

Condie (1991) has shown the relatively common occurrence of anorogenic granites in Archaean terrains, even though most of the granites cited by him, as representative of this group, display geochemical characteristics clearly distinct from those observed in Proterozoic anorogenic granites worldwide. On the other hand, Moore *et al.* (1993) described an Archaean rapakivi granite-anorthosite-rhyolite complex in Southern Africa.

This paper presents geochemical data of the Estrela Granite Complex, in an attempt to contribute to the discussion about the significance of A-type granites in Archaean terrains. Structural, microstructural and petrographic

aspects of the Estrela Granite Complex, as well as Rb-Sr geochronological data have been further discussed by Barros (1991), Barros *et al.* (1992) and Barros and Dall'Agnol (in press).

GEOLOGICAL ASPECTS

The Estrela Granite Complex consists of an ellipsoidal batholith which outcrops at the southeastern border of the Amazonian Craton (Almeida *et al.*, 1981), in the Carajás Mining Province (Fig. 1). Initially, this complex had been correlated with the Proterozoic anorogenic granites due to its essentially monzogranitic composition and strong positive radiometric anomalies (Hirata *et al.*, 1982; Meireles *et al.*, 1984; DOCEGEO, 1988). Araújo *et al.* (1988) identified ductile shear structures in these rocks and suggested the name "Estrela Gneiss". Araújo *et al.* (1988) and Costa *et al.* (1990) assumed that this complex was strongly deformed by the Itacaiúnas Shear Belt, during Late Archaean times. Costa *et al.* (1990) described a major strike-slip system which affected this granitoid body. Nevertheless, considering the composite nature of this batholith, its banded aspect in some outcrops and the nature of the deformational processes, probably related to its emplacement (Barros *et al.*, 1994), it is suggested here to name it a *granite complex*, in agreement with the Brazilian Stratigraphic Nomenclature Code (Petri *et al.*, 1986), so avoiding referring to it as gneiss.

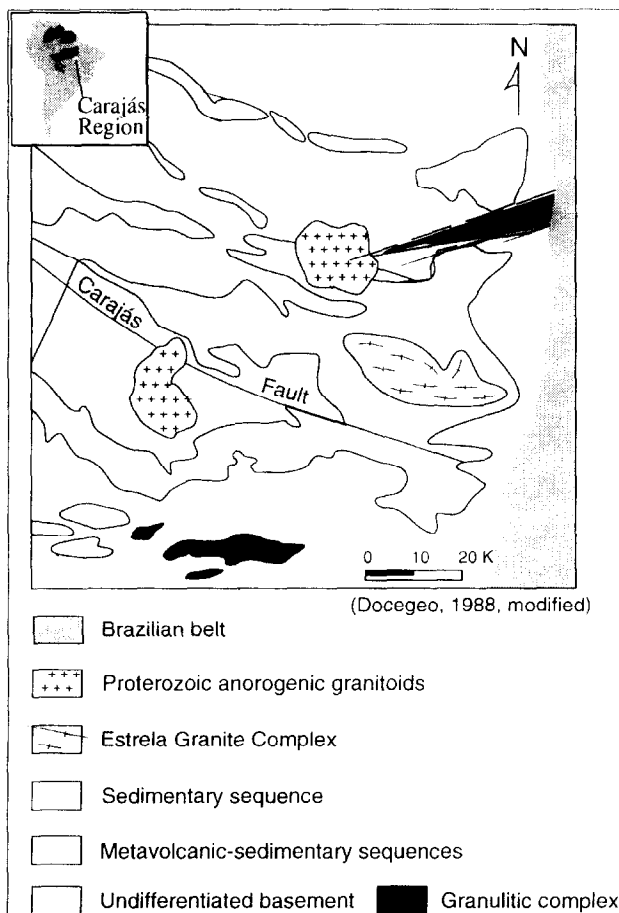


Fig. 1. Simplified geological map of the Carajás region.

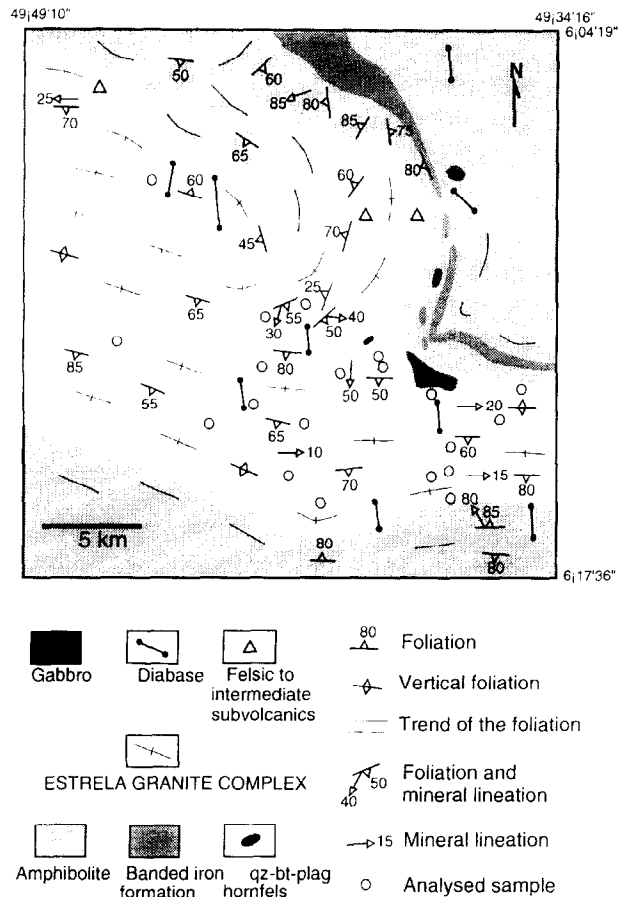


Fig. 2. Geological map of the Estrela Granite Complex.

The Estrela Granite Complex (Fig. 2) is surrounded by supracrustal rocks, metamorphosed under medium- to high-grade conditions, belonging to the Itacaiúnas Supergroup (DOCEGEO, 1988). An U-Pb zircon age of 2.76 Ga has been obtained in rocks of this supergroup, in the Carajás region (Machado *et al.*, 1991). To the north, the host rocks are dominantly amphibolites with subordinate occurrences of banded iron formations and minor lenses of garnet- and tourmaline-bearing quartz-biotite-plagioclase hornfels. The amphibolites present granoblastic and granonematoblastic textures (*cf.* Bard, 1990). Sometimes a well-defined foliation outlined by oriented plagioclase and amphibole crystals is observed. Large xenoliths of amphibolite and more rarely of hornfelsed pelites, similar in texture and mineralogy to the host rocks, are found within the batholith. To the south of the massif, the host rocks are dominantly amphibolites. Biotite-amphibole-plagioclase-garnet-quartz gneisses and quartz-chlorite-sericite schists are locally present. These rocks may be strongly strained, showing a well-defined foliation and stretching lineations. Locally, syn-tectonic recrystallization is indicated by snow-ball garnet porphyroblasts.

Two major structural domains have been identified in the batholith. The largest one is found in the western and southern parts of the body, and is characterized by a nearly E-W-trending foliation dipping 70° south. Sinistral ductile strike-slip shear-zones have been described in this domain. The second structural domain, characterized by a NNE-SSW-trending foliation, occurs in the northeastern part of the massif (Fig. 2).

The granitoids exhibit a strong plano-linear fabric (locally mylonitic), defined by the preferred orientation of their minerals. The planar fabric may also be outlined by alternating discontinuous quartzofeldspathic and mafic-enriched levels (Barros *et al.*, 1994). On the foliation surface, elongation ribbon lineations (*cf.* Mc Lelland, 1984), outlined by the preferred orientation of monomineralic aggregates, have commonly been found. Mesoscopic ptygmatic folds and tight to gentle folds, boudins and pinch-and-swell structures have also locally been observed. The microstructures and the rheological behavior of the feldspars (Tullis, 1983; Ji and Mainprice, 1990) suggest that these rocks have been subjected to temperatures higher than 500°C during the shearing (Barros, 1991; Barros and Dall'Agnol, in press).

The lithological units described above are crosscut by undated diabase dykes, small gabbroic stocks as well as by intermediate-to-felsic subvolcanic rocks.

PETROGRAPHY

The Estrela Granite Complex is essentially composed of monzogranitic rocks (*cf.* Streckeisen, 1976), although tonalitic, granodioritic and syenogranitic varieties have locally been found (Fig. 3). Only the monzogranites will be discussed below, the tonalitic, granodioritic and syenogranitic rocks sharing the same mineralogical characteristics, the K-feldspar/plagioclase ratios excepted. The monzogranites are crosscut by amphibole-bearing pegmatites and by quartzofeldspathic veins.

Monzogranites. They comprise fine- to medium-grained light-grey-coloured foliated rocks. Hornblende and biotite are the main mafic minerals, but clinopyroxene may occur in the hornblende-rich varieties. Allanite, zircon, magnetite and apatite occur in accessory amounts. A sec-

ondary mineral assemblage made up of chlorite, epidote, sphene, opaques, carbonates and stilpnomelane is locally observed.

Five facies have been distinguished on the basis of modal mineral proportions, namely, hornblende-pyroxene monzogranites, hornblende monzogranites, biotite-hornblende monzogranites, hornblende-biotite monzogranites and biotite monzogranites (Fig. 3). The Q-A-P plot show a clear dominance of monzogranitic compositions in the complex, while the Q-(A+P)-M plot demonstrates that the rocks in which biotite is the main mafic phase present lower modal contents of mafic minerals in comparison with the relatively hornblende-rich rocks (Fig. 3).

The above mentioned petrographic facies show a regular distribution over the batholith so that, with some exceptions, biotite monzogranites concentrate in its western part, while the hornblende monzogranites occur preferentially in the eastern one. Rocks containing both biotite and hornblende are found between these two main petrographic domains defining apparently a transitional zone. The pyroxene-bearing monzogranites are found in association with the hornblende-rich facies.

The main features of minerals are briefly described below.

Quartz shows wavy extinction, kink bands, subgrains and neoblasts with increasing deformation. In mylonitic rocks, recrystallization and tectonic grain size reduction is more important.

Microcline occurs as medium- to fine-grained weakly-perthitic crystals which exhibit a preferred orientation in the more intensely deformed rocks. Strain has produced undulatory extinction as well as recrystallization of the margins of the porphyroclasts yielding core and mantle textures as described by some authors (White *et al.*, 1980; White and Mawer, 1986).

Plagioclase occurs as anhedral porphyroclasts (An₁₅₋₁₈) which show locally undulatory extinction and kink bands, as well as mantle and core textures. Ribbons of plagioclase have also been observed. Small neoblasts of plagioclase (An₈₋₁₀) are more abundant in the mylonites.

Amphibole is a green-to-bluish-green iron-rich hornblende which has very low biaxial angle. Microprobe analyses revealed very high FeO (25.56%-33.01%) and low MgO (0.38%-3.79%) contents characteristic of ferro-pargasite and hornblende ferro-pargasite according to Leake (1978). The hornblende Fe²⁺/(Fe²⁺+Mg) ratios are very high (0.86-0.97). The porphyroclasts exhibit a stress-induced preferred orientation and dynamic recrystallization. Locally, the amphiboles underwent partial alteration to epidote, chlorite, opaques and stilpnomelane.

When present, *clinopyroxene* occurs as relict crystals partly replaced by fine-grained hornblende neoblasts. The clinopyroxene has the composition of ferrosalite, with high FeO (18.78%-20.60%) and CaO (21.96%-22.71%), and low MgO (6.02%-6.63%) contents.

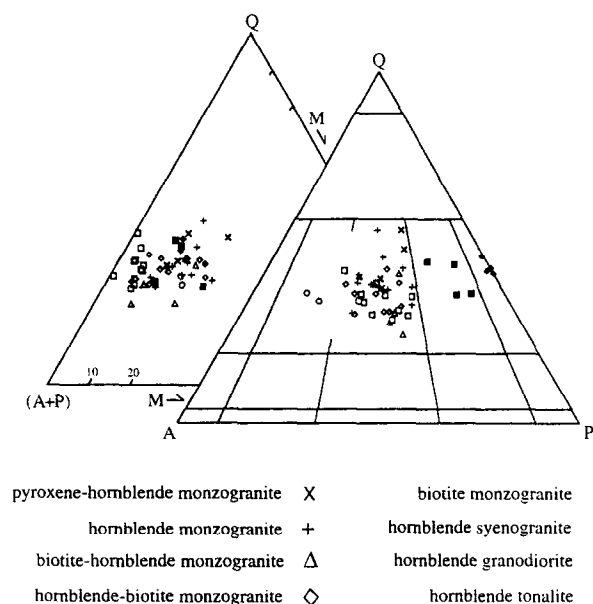


Fig. 3. Q-A-P and Q-(A+P)-M plots for the Estrela Granite Complex.

Table 1. Major (wt.%) and trace element (ppm) analyses of the Estrela Granite Complex

	Biotite monzogranite				Biotite-hornblende monzogranite				Hornblende-biotite monzogranite	
	III-22	IV-74	IV77	CRN33	CN33A	CN40	V118	CN100	CN104	V162
SiO ₂	71.78	72.16	74.69	75.06	71.67	73.12	72.10	72.74	70.81	69.73
TiO ₂	0.27	0.26	0.14	0.16	0.22	0.35	0.27	0.28	0.32	0.64
Al ₂ O ₃	13.37	13.42	13.38	13.74	13.23	13.64	13.64	13.69	13.65	11.60
Fe ₂ O ₃	1.43	1.40	1.19	0.51	1.12	1.67	1.09	1.33	2.12	3.92
FeO	2.72	2.08	1.44	1.79	3.44	2.83	2.59	2.51	3.69	4.57
MnO	0.03	0.02	0.01	0.01	0.03	—	0.02	0.02	0.02	0.03
MgO	0.18	0.13	0.06	0.09	0.13	0.12	0.25	0.19	0.12	0.14
CaO	1.43	1.32	1.08	1.05	1.25	1.53	1.48	1.39	1.61	2.09
Na ₂ O	3.42	3.36	3.42	3.07	3.48	2.72	3.12	2.76	3.48	2.96
K ₂ O	4.87	4.76	5.65	5.33	4.58	3.92	4.74	4.83	3.98	4.25
P ₂ O ₅	0.07	0.07	0.06	0.07	0.07	0.08	0.09	0.08	0.10	0.12
L.O.I. ⁽¹⁾	0.77	0.65	0.32	0.50	0.84	0.67	0.72	0.72	1.09	0.60
Total	100.34	99.63	100.44	101.38	100.06	100.65	100.11	100.54	100.99	100.65
Rb	237	200	223	259	331	287	255	265	131	168
Sr	66	81	55	63	62	64	83	84	95	47
Y	86	65	13	42	88	102	61	50	84	131
Zr	273	260	146	147	210	258	237	217	255	640
Nb	33	29	21	30	35	45	27	28	30	34

⁽¹⁾L.O.I. = Loss on ignition corrected using the formula of Lechlers & Desilets (1987).

Biotite occurs as fine-grained, weakly to strongly oriented platelets defining discontinuous layers alternating with quartzofeldspathic ones. This mineral shows a brownish-green color and, sometimes, incipient chloritization. Microprobe analyses show very high FeO (32.22%–37.32%) and very low MgO (0.61%–2.19%) contents, and thus high Fe²⁺/(Fe²⁺+Mg) ratios (0.86–0.97). The chemical compositions of the biotite from the Estrela Granite Complex are comparable to those from alkaline series (Nachit *et al.*, 1985).

Hornblende-bearing pegmatites. These rocks are preferentially associated with the hornblende-enriched monzogranites and have granitic composition. They occur as decimetre to metre-thick veins conformable or cutting across the host-rock foliation. The microstructures are similar to those observed in the monzogranites. The amphibole megacrysts (up to five centimeters in length) are optically and chemically similar to the ferro-pargasites found in the host-monzogranite.

Quartzofeldspathic veins. These hololeucocratic, medium-to fine-grained, centimetre-thick veins are widespread in the Estrela Granite Complex. They are either conformable to the monzogranite foliation, or discordant and generally strongly folded.

GEOCHRONOLOGY

A whole rock Rb-Sr age of 2527 ± 34 Ma ($I_{Sr} = 0.70188 \pm 0.00197$) was obtained for the Estrela Granite Complex (Barros *et al.*, 1992). This age has been interpreted as a minimum age, probably related to the opening of the Rb-Sr system during the development of ductile shear zones. However, it is not very different from the U-Pb zircon age (2573 ± 2 Ma) obtained by Machado *et al.* (1991) for the Old Salobo Granite displaying petro-

graphic and geochemical features (Lindenmayer, 1990; Machado *et al.*, 1991) rather similar to those of the Estrela Granite Complex. It is, therefore, possible that both granites are related to a single magmatic event in the Carajás region, and that the Estrela Granite Complex Rb-Sr age may not significantly differ from its age of crystallization.

GEOCHEMISTRY

Twenty samples comprising monzogranites (17), syenogranite (1) and pegmatites (2), representative of the main facies identified in the massif, have been selected and analysed for major and trace elements in the laboratories of the Geosciences Center (University of Pará, Belém, Brazil). K, Na, Mg and Mn have been analysed by atomic absorption, whereas Si, Al, Ca, Fe_{total}, Ti, P, Rb, Sr, Y, Zr and Nb have been determined by X-ray fluorescence (XRF). XRF analyses have been calibrated against NIM-G, NIM-L and NIM-D standards. FeO has been determined by titration with K₂Cr₂O₇. Volatile contents, determined by means of heating at 1,000°C, have been corrected after calculations with Lechlers and Desilets (1987) formula and are expressed as loss on ignition (L.O.I.).

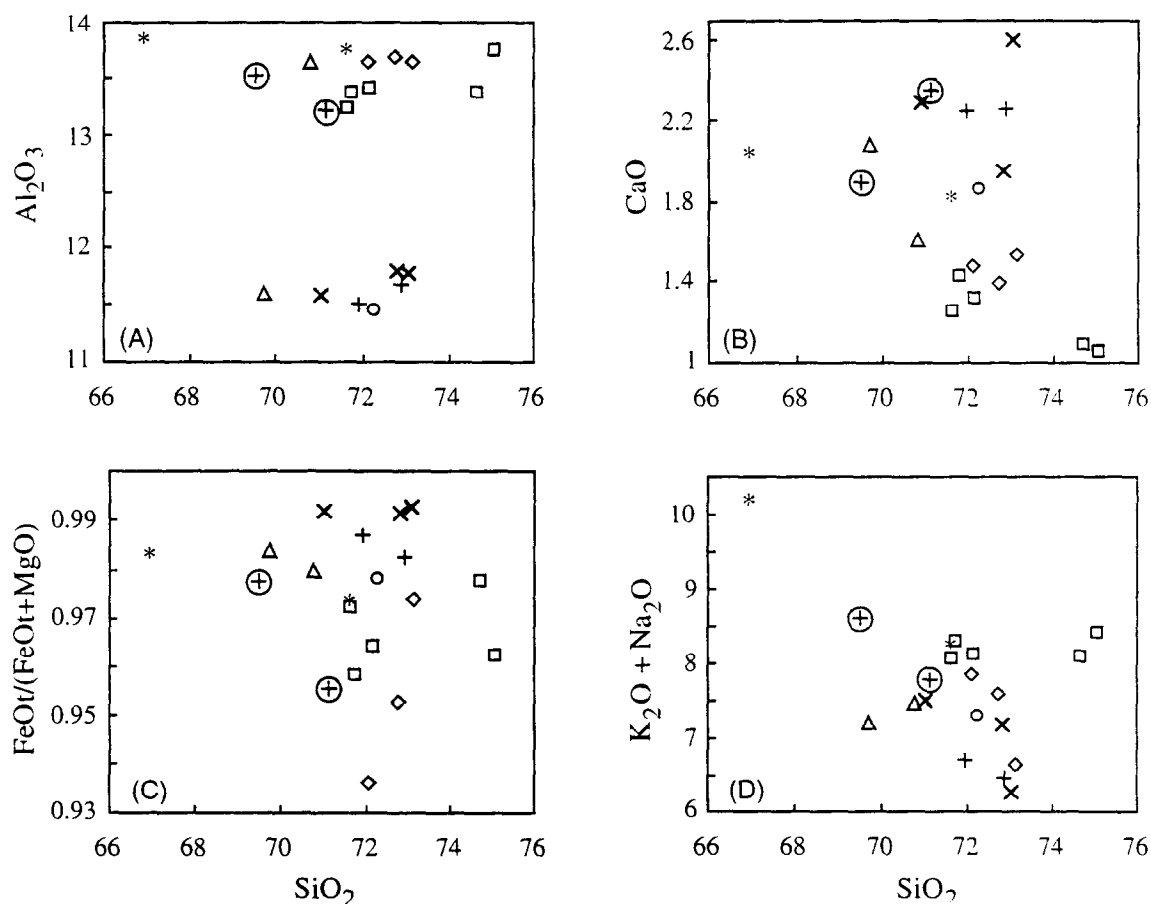
Chemical data (Table 1) and Harker diagrams (Figs. 4A–D) show that the Estrela Granite Complex has moderate and relatively homogeneous SiO₂ contents (average of 71.85%). Alumina-rich (Al₂O₃ = ~13.5%) and alumina-poor monzogranites (Al₂O₃ = ~11.5%) have been distinguished (Fig. 4A). The first weakly peraluminous group corresponds to monzogranites in which biotite is the main mafic phase. In the rocks of the second metaluminous group, hornblende is always the main mafic mineral. All hornblende monzogranites, syenogranites and pegmatites are metaluminous. However, two samples of hornblende monzogranite (VI-11 and VIII-14), the hornblende syenogranite and the hornblende pegmatites have relatively high Al₂O₃ contents. This

Table 1. — (Continued)

Hornblende pegmatite		Hornblende syenogranite		Hornblende monzogranite			Hornblende-pyroxene monzogranite		
CN23A	CRN9	CRC8D	VII1	VIII14	VIII75	VIII76	VIII16	VIII22	VIII82
66.95	71.64	72.28	69.52	71.13	72.88	71.94	73.05	72.81	71.03
0.39	0.23	0.57	0.38	0.72	0.59	0.57	0.58	0.55	0.59
13.86	13.77	11.44	13.53	13.21	11.69	11.50	11.78	11.80	11.59
3.00	1.10	2.27	1.81	1.08	2.34	2.78	1.86	2.20	1.59
4.16	2.29	4.37	3.00	2.15	3.81	4.09	3.58	3.51	3.23
0.03	0.02	0.03	0.03	0.03	0.03	0.03	0.04	0.06	0.05
0.12	0.09	0.15	0.11	0.15	0.11	0.09	0.04	0.05	0.04
2.05	1.81	1.86	1.90	2.35	2.26	2.25	2.60	1.95	2.32
2.91	3.54	1.72	3.76	3.82	3.89	3.14	2.90	3.10	3.45
7.29	4.73	5.56	4.86	3.94	2.58	3.57	3.37	4.07	4.05
0.15	0.08	0.08	0.09	0.16	0.08	0.08	0.09	0.08	0.08
0.92	0.47	0.88	0.69	0.46	0.43	0.57	0.49	0.43	0.43
101.83	99.77	101.21	99.68	99.20	100.68	200.61	100.38	100.61	98.45
151	94	87	182	144	46	66	108	84	117
75	151	27	85	166	47	33	126	49	92
156	48	79	90	76	109	118	153	106	404
80	92	505	376	500	546	631	589	545	564
33	17	23	34	32	31	31	36	29	38

appears both in the Al_2O_3 vs. SiO_2 (Fig. 4A) and the A-B (Fig. 5) diagrams. Compared to the Al_2O_3 -rich rocks, the Al_2O_3 -poor ones show relatively higher TiO_2 , $(\text{Fe}_2\text{O}_3+\text{FeO})$ and CaO contents, reflecting higher modal contents of mafic phases and the predominance of hornblende (Fig. 4B).

All analysed samples display very low MgO contents and extremely high $\text{FeO}_t/(\text{FeO}_t+\text{MgO})$ ratios (Fig. 4C), at the opposite to what is normally seen in the Archaean calc-alkaline and trondhjemite series (Condie, 1981; Martin, 1987; Sylvester, 1994). These ratios are slightly higher in



Figs 4. (A) Al_2O_3 vs. SiO_2 , (B) CaO vs. SiO_2 , (C) $[\text{FeO}_t/(\text{FeO}_t+\text{MgO})]$ vs. SiO_2 and (D) $\text{K}_2\text{O}+\text{Na}_2\text{O}$ vs. SiO_2 plots for the Estrela Granite Complex. Symbols same as in Fig. 3; (*) = hornblende-bearing pegmatites, (⊕) = Al_2O_3 -enriched metaluminous hornblende monzogranites.

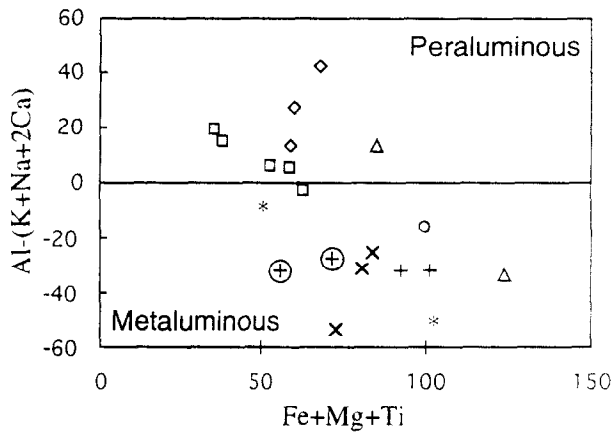


Fig. 5. A=Al-(K+Na+2Ca) vs. B=Fe+Mg+Ti plot (Debon and Le Fort, 1988) for the Estrela Granite Complex. The two parameters are in milliequivalents for 100 mg of rock. Symbols same as in Fig. 4.

the metaluminous group than in the peraluminous one. In a pegmatite sample (CN23A; Table 1) rich in hornblende megacrysts, the $\text{Fe}_2\text{O}_3+\text{FeO}$ contents (7.16%) are remarkably higher.

The $\text{K}_2\text{O}+\text{Na}_2\text{O}$ contents of the Estrela Granite Complex (Fig. 4D) are normal for monzogranites, but the K_2O contents are much higher than those observed in the Archaean TTG granitoids (Martin, 1987). K_2O is higher in the peraluminous monzogranites, pegmatites and syenogranites. Except for one sample (VIII-75), the $\text{K}_2\text{O}/\text{Na}_2\text{O}$ ratios are greater than one. The chemical analyses plot within the granite field in the An-Ab-Or normative diagram (Fig. 6) of Barker (1979). In this diagram, the Estrela Granite Complex and the Mata Surrão Granite (Rio Maria region) samples plot in areas largely coincident, reflecting their common monzogranitic composition. On the other hand, the Rio Maria Granodiorite and the Arco Verde Tonalite samples plot in distinct fields (Fig. 6).

The Estrela Granite Complex also exhibits high and,

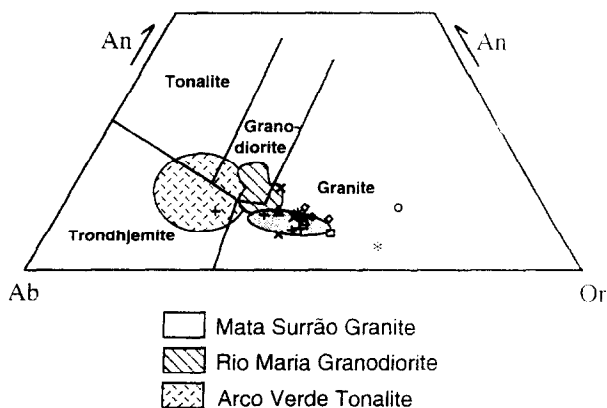


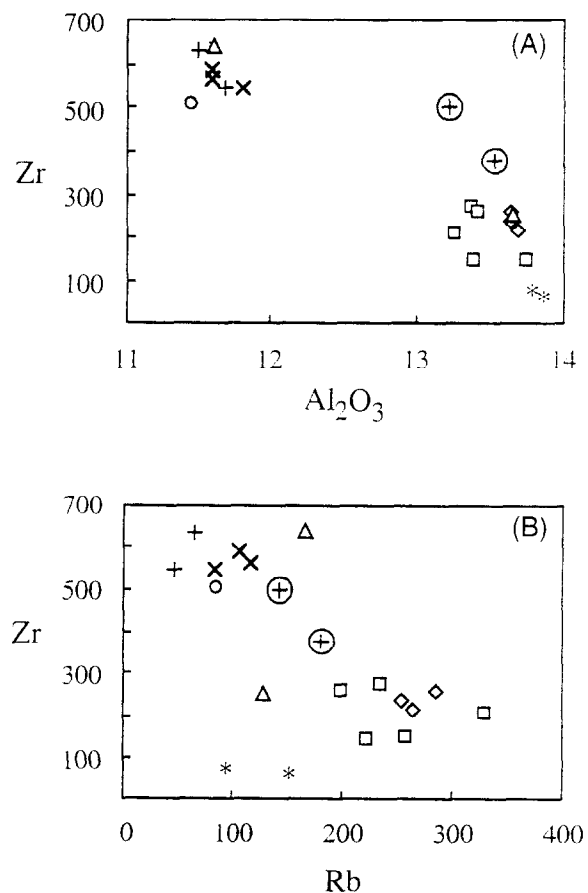
Fig. 6. An-Ab-Or diagram (Barker, 1979), showing the similar behavior of the Estrela Granite Complex and Mata Surrão Granite (Duarte 1992), contrasting with the Rio Maria Granodiorite (Medeiros, 1987) and Arco Verde Tonalite (data from Althoff *et al.*, 1994). Symbols same as in Fig. 4.

sometimes, exceptionally high Zr, Y and Nb contents compared with typical values of Archaean granitoids. The peraluminous and metaluminous groups are clearly discriminated in the Al_2O_3 -Zr plot (Fig. 7A), with average Zr contents of 550 ppm and 250 ppm, respectively. The two hornblende monzogranite samples rich in Al_2O_3 show Zr contents near to those of the peraluminous group. The Y behavior is similar to that of Zr, although not so contrasted. Nb values are relatively homogeneous, oscillating around 30 ± 10 ppm (Table 1).

Sr values are generally lower than 100 ppm (Table 1) and no clear difference between the two monzogranite groups is found. Rb contents are extremely variable and increase significantly from the Al_2O_3 -poor to the Al_2O_3 -rich rocks. In the Rb-Zr plot (Fig. 7B), most of the metaluminous and peraluminous monzogranites are distributed in two different domains. The ambiguous behavior of the two Al_2O_3 -rich hornblende monzogranite samples is also evident. The pegmatites show very low Zr concentrations, suggesting previous fractionation of zircon.

TYOLOGY

The high $\text{K}_2\text{O}+\text{Na}_2\text{O}$ contents, the extremely high $\text{FeO}_1/(\text{FeO}_1+\text{MgO})$ ratios, and the elevated high field strenght elements (HFSE) contents of the Estrela Granite Complex

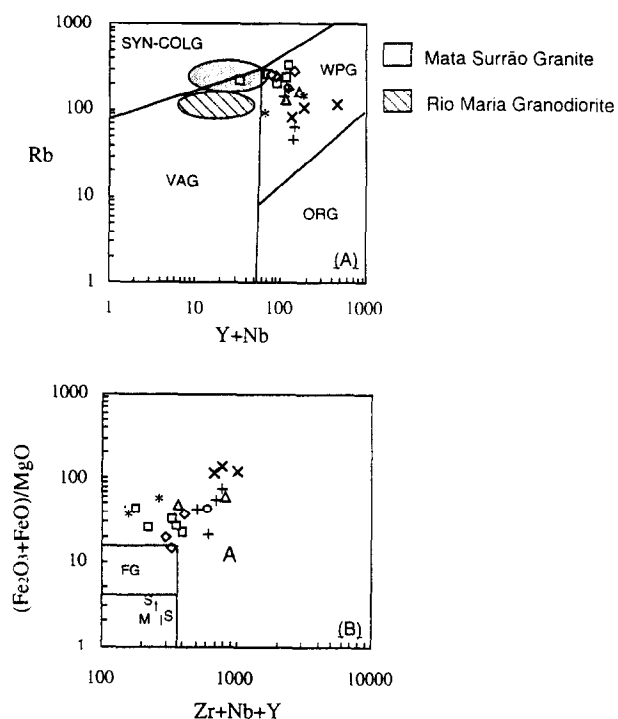


Figs 7. (A) Al_2O_3 vs. Zr and (B) Rb vs. Zr plots for the Estrela Granite Complex showing two contrasted rock groups. Symbols same as in Fig. 4.

as well, indicate strong geochemical affinities with A-type granites as defined by Loiselle and Wones (1979), Collins *et al.* (1982) and Whalen *et al.* (1987).

The diagrams proposed by Pearce *et al.* (1984) have been used to support the discussion concerning the typology of the studied rocks, in spite of the fact that those diagrams have originally been proposed for characterizing Phanerozoic granites, as well as of the difficulties in distinguishing anorogenic and post-tectonic alkaline granites only from their geochemical signatures (Sylvester, 1989). For instance, the Rb-(Y+Nb) and Nb-Y plots are useful to discriminate within-plate granites from other types of granites. In the Rb-(Y+Nb) plot (Fig. 8A), the Estrela Granite Complex data cluster in the within-plate-granite field, whereas representative Archaean granitoids from the Rio Maria region (Rio Maria Granodiorite and Mata Surrão Granite) plotted for comparison, fall within the volcanic-arc-granite and syn-collisional-granite fields.

Whalen *et al.* (1987), discussing the A-type granites geochemistry, proposed several diagrams to discriminate them from I, S, and M-type granites. The limited amount of available analytical data for the Estrela Granite Complex hinders the use of some of these diagrams. Nevertheless, the $[(\text{Fe}_2\text{O}_3 + \text{FeO})/\text{MgO}] - (\text{Zr} + \text{Nb} + \text{Y})$ plot is presented here (Fig. 8B). Even though Ce contents have not been analysed, it can be noted that the Estrela Granite Complex



Figs 8. (A) (Y+Nb) vs. Rb diagram (Pearce *et al.*, 1984) for the Estrela Granite Complex showing affinities with the Within-Plate Granites (WPG). ORG= Ocean Ridge granites; VAG= Volcanic Arc granites; SYN-COLG= Syn-Collisional granites. (B) (Zr+Nb+Y) vs. $[(\text{Fe}_2\text{O}_3 + \text{FeO})/\text{MgO}]$ plot (Whalen *et al.*, 1987) for the Estrela Granite Complex, showing affinities with the A-type granites. Note that Ce data are not available. FG = fractionated granites; A, I, M and S are the average of the A-, I-, M- and S-type granites (Whalen *et al.* op. cit.). Symbols same as in Fig. 4.

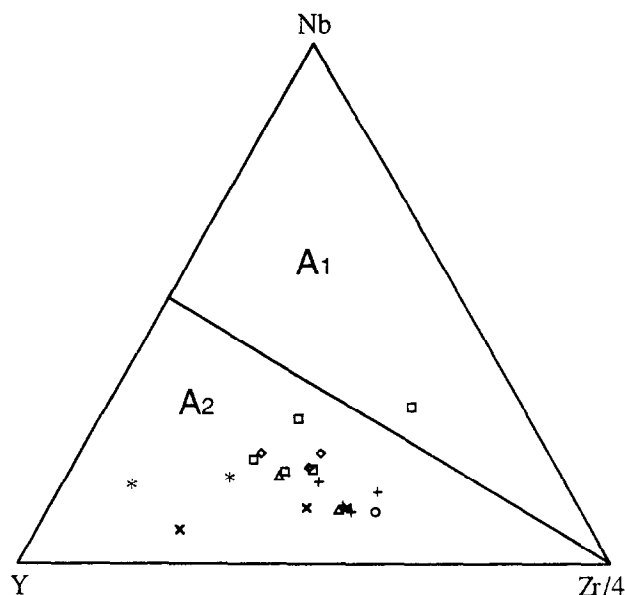


Fig. 9. Nb-Y-Zr/4 plot for the Estrela Granite Complex, showing affinities with the A₂-type crustal granites of Eby *et al.* (1992); A₁ = mantle derived granites. Symbols same as in Fig. 4.

has a geochemical signature entirely different from the I, S and M-type granites, but similar to that of the A-type granites.

On the basis of the A-type geochemical signature of the Estrela Granite Complex, the Nb-Y-Zr/4 plot with the mantle-derived (A₁) and crustal-source (A₂) fields of Eby *et al.* (1992), has been used (Fig. 9). The analysed rocks (a sample of biotite monzogranite, excepted) plot in the A₂ field, suggesting an important crustal contribution or even an essentially crustal origin for its parental magma.

The new chemical classification proposed by Sylvester (1994) for alkaline granites defines two Phanerozoic subtypes (ALK-1 and ALK-2) and their Archaean counterparts (ALK-3 and ALK-4), as well. The major and trace elements data for the Estrela Granite Complex are rather similar to the ALK-3 subtype, in spite of the fact that the Y and Zr contents (mainly of the metaluminous rocks) are higher and comparable to those of the ALK-1 Phanerozoic granites.

PETROGENESIS

The available data do not allow definitive conclusions about the petrogenesis of these rocks. Nevertheless, some preliminary ideas on their likely magma source can be presented here. The geochemical signature of the studied rocks, particularly their extremely-high $\text{FeO}_t/(\text{FeO}_t + \text{MgO})$ ratios, their quite homogeneous silica contents and their plot in the A₂ crustally-derived granite field (Eby, 1992) favour essentially a crustal origin for the rocks under discussion.

The low initial $^{87}\text{Sr}/^{86}\text{Sr}$ initial ratios of the Estrela Granite Complex could be explained either by the partial melting of crustal rocks with short crustal-residence time,

or by partial melting of crustal material with low Rb/Sr ratios, or even by partial melting of source rocks with an important mantle contribution (Barros *et al.*, 1992). However, Rb and Sr data must be considered carefully because these elements may present a mobile behavior in response to the ductile deformation and/or hydrothermal alteration. Another point to be considered is that the coincidence between Rb-Sr age of the complex (Barros *et al.*, 1992) and that of its magmatic crystallization is not yet demonstrated.

Three main models have been proposed favouring a crustal source for A-type granite magmas: (1) partial melting of relatively dry meta-igneous rocks of granodiorite to tonalite compositions (Anderson *et al.*, 1980; Anderson and Bender, 1989; Creaser *et al.*, 1991); (2) melting of residual granulitic rocks from which an I-type melt had previously been extracted (Collins *et al.*, 1982; Clemens *et al.*, 1986); (3) partial melting of igneous rocks metamorphosed under granulite facies conditions but without any previous extraction of an I-type magma (Bickle *et al.*, 1989; Cerny *et al.*, 1987; Sheraton and Black, 1988).

The very high Y concentrations found in these granites suggest that mafic phases rich in Y contributed to the melt to concentrate this element in the liquid phase, as suggested by Sheraton and Black (1988) and Sylvester (1989). Such a source relatively enriched in Y-bearing mafic phases could also account for the high Y contents found in the Estrela Granite Complex monzogranites, mainly in the metaluminous varieties.

The existence of a gap between the peraluminous and metaluminous groups can not be easily explained by magmatic differentiation alone. Probably, the rocks of the Complex might have been generated from more than one melt. These melts could reflect differences in the magma-source compositions as well as in the rates of melting. The metaluminous group, compared to the peraluminous one, is enriched in amphibole and mafic phases as well as in high field strength elements. This is thought to be evidence that during magma generation, the temperatures had been high enough to melt considerable proportions of mafic phases. The peraluminous monzogranites might have been generated from a relatively lower-temperature melt, derived from a more leucocratic and alkali-feldspar-enriched source, possibly containing biotite as an additional mafic phase. High temperatures, generally accepted to produce A-type granites, are thought to favor zircon solubility, leading to the presence of high Zr (and related elements) concentrations in the melt (Anderson and Bender, 1989; Sheraton and Black, 1988).

The petrogenetical and geochemical data discussed above suggest that a petrogenetic model involving partial melting of crustal rocks at high-temperature conditions could be expected to generate magmas with the characteristics found in the Estrela Granite Complex. The generation of granitoid magmas enriched in HFSE by means of repeated small-extent partial melting of depleted granulitic rocks is hardly acceptable since the amount of HFSE is expected to be excessively low in the restite (Creaser *et al.* 1991). Anyway, it is important to remember that the A-type

granites can have a complex petrogenetic history, including crustal or subcontinental mantle components (Eby, 1992), halogen-bearing complexes due to the breakdown of biotites and/or amphiboles (Cerny *et al.*, 1987; Clemens *et al.*, 1986; Moorbath *et al.*, 1981) or else partial melting of metasomatized source rocks (Sylvester, 1994), and any interpretation of their origin should not be oversimplified.

CONCLUSIONS

The Estrela Granite Complex consists of an heterogeneously deformed Archaean monzogranitic batholith, where a large facies variation, mainly defined by the nature and abundance of the mafic phases, is observed. Chemical data demonstrate the alkaline affinities of the studied rocks and allowed them to be subdivided into two distinct groups with respect to the Al_2O_3 contents. The group of granites poor in Al_2O_3 is metaluminous while that rich in Al_2O_3 is weakly peraluminous. Both present chemical affinities with A-type granites and may be classified as such. The Estrela Granite Complex geochemical signature is very different from those observed in the granitoid rocks described in the Archaean granite-greenstone terrain from the Rio Maria region, where calc-alkaline and trondhjemitic series are predominant (Medeiros, 1987; Dall'Agnol *et al.*, 1987; Duarte, 1992; Althoff *et al.*, 1994).

The Estrela Granite Complex represents an unequivocal example of Archaean A-type granite magmatism. The chemical data suggest that partial melting of a crustal source composed of meta-igneous or undepleted granulitic rocks could be able to generate the Estrela magmas.

The presence of the Old Salobo Granite (Lindenmayer, 1990; Lindenmayer *et al.* 1994) in the Salobo area, north of the Serra dos Carajás region, bearing many similarities with the Estrela Granite Complex, demonstrates that the A-type granitoids played an important role in the Archaean evolution of the Carajás Mining Province.

Acknowledgements — This research was supported by: Conselho Nacional de Desenvolvimento Científico e Tecnológico (CNPq); PADCT-FINEP (4/3/87/0911/00 and 6.5.92.0025.00) and Companhia Vale do Rio Doce (CYRD-UFPA-FADESP). The Centro de Geociências (UFPA), as well the technical staff of its geochemistry laboratories are also acknowledged. We wish to express gratitude to Prof. Ian McReath and Prof. Ramon Capdevila for the unvaluable comments on the manuscript. We wish to thank J. Jabbori, L. Aillères, B. Gérard and F. Althoff for helping in computer programs.

REFERENCES

- Almeida, F.F.M.; Hasui, Y.; Brito-Neves, B.B.; Fuck, R.A. 1981. Brazilian structural provinces: an introduction. *Earth-Science Reviews* **17**, 1–29.
- Althoff, F.J.; Barbey, P.; Boullier, A.M.; Dall'Agnol, R. 1994. Regime tectônico e composição dos granitóides arqueanos da região de Marajoara. *Resumos expandidos, IV Simpósio de Geologia da Amazônia, Belém*, 291–294.
- Anderson, J.L. and Bender, E.E. 1989. Nature and origin of Proterozoic A-type granitic magmatism in the southwestern United States of America. *Lithos* **23**, 19–52.

- Anderson, J.L.; Cullers, R.L.; Van Schmus, W.R. 1980. Anorogenic Meta-luminous and Paraluminous Granite Plutonism in the Mid-Proterozoic of Wisconsin, USA. *Contributions to Mineralogy and Petrology* **74**, 311–328.
- Araújo, O.J.B.; Maia, R.G.N.; Jorge-João, X.S.; Costa, J.B.S. 1988. A Megaestruturação Arqueana da Folha Serra dos Carajás. *Anais, VII Congresso Latino-Americano de Geologia, Belém* **1**, 324–338.
- Bard, J.P. 1990. Microtextures des Roches Magmatiques et Métamorphiques. Paris, Mason, 208 p.
- Barker, F. 1979. Trondhjemite: definition, environment and hypothesis of origin. In: *Trondhjemites, Dacites and related rocks.* (edited by F. Barker) Amsterdam, Elsevier, pp. 1–12. (Developments in Petrology 6).
- Barros, C.E.M. 1991. *Evolução petrológica e estrutural do Gnaiss Estrela, Curionópolis, PA.* Unpublished thesis, Universidade Federal do Pará, Belém, 134 p.
- Barros, C.E.M. and Dall'Agnol, R. 1994. Deformação de rochas granitoides em regime dúctil: o exemplo do Gnaiss Estrela, Região de Carajás. *Revista Brasileira de Geociências* (in press).
- Barros, C.E.M.; Dall'Agnol, R.; Barbey, P.; Boullier, A.M. 1994. Le Gneiss Estrela (Craton Amazonien, Brésil): mise en place d'un pluton granitique Archéen de type A. *Anais, XV Réunion des Sciences de la Terre, Nancy*, 9.
- Barros, C.E.M.; Dall'Agnol, R.; Lafon, J.M.; Teixeira, N.P.; Ribeiro, J.W. 1992. Geologia e geocronologia Rb-Sr do Gnaiss Estrela, Curionópolis, PA. *Boletim do Museu Paraense Emílio Goeldi, Ciências da Terra* **4**, 83–102.
- Bickle, M.J.; Bettenay, L.F.; Chapman, H.J.; Groves, D.I.; McNaughton, N.J.; Campbell, I.H.; Laeter, J.R. 1989. The age and origin of younger granitic plutons of the Shaw Batholith in the Archaean Pilbara Block, Western Australia. *Contributions to Mineralogy and Petrology* **101**, 361–376.
- Cerny, P.; Fryer, B.J.; Longstaffe, F.J.; Tammemagi, H.Y. 1987. The Archean Lac du Bonnet batholith, Manitoba: Igneous history, metamorphic effects, and fluid overprinting. *Geochimica et Cosmochimica Acta* **51**, 421–438.
- Clemens, J.D.; Holloway, J.R.; White, A.J.R. 1986. Origin of an A-type granite: experimental constraints. *American Mineralogist* **71**, 317–324.
- Collins, W.J.; Beams, S.D.; White, A.J.R.; Chappell, B.W. 1982. Nature and origin of A-type granites with particular reference to southeastern Australia. *Contributions to Mineralogy and Petrology* **80**, 189–200.
- Condie, K.C. 1981. Archean Greenstone Belts. *Developments in Precambrian Geology* **3**. Elsevier, Amsterdam, 434 p.
- Condie, K.C. 1991. Precambrian granulites and anorogenic granites: are they related? *Precambrian Research* **51**, 161–172.
- Costa, J.B.S.; Teixeira, N.P.; Pinheiro, R.V.L.; Bermerguy, R.L. 1990. Os Sistemas Estruturais Transcorrentes do Cinturão Itacaiúnas na Região de Curionópolis, Leste do Estado do Pará. *Anais, "V Congresso Brasileiro de Geologia, Natal* **5**, 2345–2352.
- Creaser, R.A.; Price, R.C.; Wormald, R.J. 1991. A-type granites revisited: Assessment of a residual-source model. *Geology* **19**, 163–166.
- Dall'Agnol, R.; Bettencourt, J.S.; João, X.S.J.; Medeiros, H.; Costi, H.T.; Macambira, M.J.B. 1987. Granitogenesis in Northern Brazilian Region: A Review. *Revista Brasileira de Geociências* **17** (4), 382–403.
- Debon, F. and Le Fort, P. 1988. A cationic classification of common plutonic rocks and their magmatic associations: principles, method, applications. *Bulletin de Minéralogie* **111**, 493–510.
- DOCEGEO (Rio Doce Geologia e Mineração). 1988. Revisão Litoestratigráfica da Província Mineral de Carajás. *Anais, "V Congresso Brasileiro de Geologia, Anexo: Província Mineral de Carajás – Litoestratigrafia e Principais Depósitos Mineraiis, Belém*, 11–54.
- Duarte, K.D. 1992. *Mapeamento e petrologia do Granito Mata Surrão: um exemplo de granito "stricto sensu" arqueano.* Unpublished thesis, Universidade Federal do Pará, Belém, 217 p.
- Eby, G.N. 1992. Chemical subdivision of the A-type granitoids: petrogenetic and tectonic implications. *Geology* **20**, 641–644.
- Eby, G.N.; Krueger, H.W.; Creasy, J.W. 1992. Geology, geochronology and geochemistry of the White Mountain batholith, New Hampshire. In: *Eastern North American Mesozoic magmatism* (edited by J.H. Puffer and P.C. Ragland), pp. 379–398. Geological Society of America Special Paper, 268.
- Ferreira, Z.C.A. and Serfaty, S. 1988. Resultados preliminares de alguns elementos-traço no "Granito" Parauapebas (Estrela), SE do Pará. *"V Congresso Brasileiro de Geologia, Belém* **3**, 1117–1131.
- Hirata, W.K.; Rigon, J.C.; Kadekaru, K.; Cordeiro, A.A.C.; Meireles, E.M. 1982. Geologia Regional da Província Mineral de Carajás. *Anais, I Simpósio de Geologia da Amazônia, Belém* **1**, 100–110.
- Huhn, S.B.; Santos, A.B.S.; Amaral, A.F.; Ledshan, E.J.; Gouvea, J.L.; Martins, L.P.B.; Montalvão, R.M.G.; Costa, V.G. 1988. O terreno granito-"greenstone" da região de Rio Maria. *Anais, "V Congresso Brasileiro de Geologia, Belém* **3**, 1438–1452.
- Ji, S. and Mainprice, D. 1990. Recrystallization and fabric development of plagioclase. *Journal of Geology* **98**, 65–79.
- Jorge João, X.S.; Lobato, T.A.M.; Marques, M.T.G. 1991. Litogeoquímica — petroquímica. In: *Programa Levantamentos Geológicos Básicos do Brasil. Programa Grande Carajás. Serra dos Carajás. Folha SB.22-Z-A. Estado do Pará. Texto Explicativo* (edited by O.J.B. Araújo and R.G.N. Maia), pp. 79–95, DNPM/CPRM, Brasília.
- Leake, B.E. 1978. Nomenclature of amphiboles. *Canadian Mineralogy* **16** (4), 501–520.
- Lechlers, P.J. and Desilets, M.O. 1987. A review of the use of loss on ignition as a measurement of total volatiles in whole-rock analysis. *Chemical Geology* **63**, 341–344.
- Leite, A.A.S. and Dall'Agnol, R. 1994. Estratigrafia e aspectos geológicos da região de ocorrência do Granito Xinguara (SE do Pará). *Resumos expandidos, IV Simpósio de Geologia Amazônia, Belém*, 325–327.
- Lindenmayer, Z.G. 1990. *Salobo Sequence, Carajás, Brazil: geology, geochemistry and metamorphism.* Unpublished thesis, University of Western Ontario, 406 p.
- Lindenmayer, Z.G.; Fyfe, W.S.; Bocalon, V.L.S. 1994. Nota preliminar sobre as intrusões granitoides do depósito de cobre do Salobo, Carajás. *Acta Geologica Leopoldensia* **40** (27), 153–184.
- Loiselle, M.C. and Wones, D.R. 1979. Characteristics of anorogenic granites. *Geological Society of America Abstracts with Programs* **11**, 468.
- Macambira, M.J.B. 1992. *Chronologie U-Pb, Rb-Sr, K-Ar et croissance de la croûte continentale dans l'Amazonie du sud-est; exemple de la région de Rio Maria. Province de Carajás, Brésil* Unpublished thesis, Université de Montpellier, 212 p.
- Macambira, M.J.B. and Lafon, J.M. 1994. Geocronologia da Província Mineral de Carajás; síntese dos dados e novos desafios. *Resumos expandidos, IV Simpósio de Geologia da Amazônia, Belém*, 339–342.
- Machado, N.; Lindenmayer, Z.; Krogh, T.H.; Lindenmayer, D. 1991. U-Pb geochronology of Archean magmatism and basement reactivation in the Carajás area, Amazon shield, Brazil. *Precambrian Research* **49**, 329–354.
- Mc Lelland, J.M. 1984. The origin of ribbon lineation within the southern Adirondacks, USA. *Journal of Structural Geology* **6** (1/2), 147–157.
- Martin, H. 1987. Petrogenesis of Archean trondhjemites, tonalites, and granodiorites from eastern Finland: major and trace element geochemistry. *Journal of Petrology* **28**, 921–953.
- Medeiros, H. 1987. *Petrologia da porção leste do batólito granodiorítico de Rio Maria, sudeste do Estado do Pará.* Unpublished thesis, Universidade Federal do Pará, Belém, 184 p.

- Medeiros, H. and Dall'Agnol, R. 1988. Petrologia da porção leste do Batólito Granodiorítico Rio Maria, Sudeste do Pará. "V Congresso Brasileiro de Geologia, Belém 3, 1488–1499.
- Meireles, E.M.; Hirata, W.K.; Amaral, A.F.; Medeiros Filho, C.A.; Gato, V.C. 1984. Geologia das folhas Carajás e Rio Verde, Província Mineral Carajás, Estado do Pará. *Anais, "III Congresso Brasileiro de Geologia, Rio de Janeiro 5, 2164–2174.*
- Moorbath, S.; Taylor, P.N.; Goodwin, R. 1981. Origin of granitic magma by crustal remobilisation: Rb-Sr and Pb/Pb geochronology and isotope geochemistry of the late Archaean Qôrqu Granite Complex of southern West Greenland. *Geochimica et Cosmochimica Acta* **45**, 1051–1060.
- Moore, M.; Davis, D.W.; Robb, L.J.; Jackson, M.C.; Grobler, D.F. 1993. Archaean rapakivi granite — anorthosite — rhyolite complex in the Witwatersrand basin hinterland, southern Africa. *Geology* **21**, 1031–1034.
- Nachit, H.; Razafimahefa, N.; Stussi, J.M.; Carron, J.P. 1985. Composition chimique des biotites et typologie magmatique des granitoïdes. *Compte Rendus de l'Académie de Sciences de Paris*, **301**, II, (11), 813–818.
- Pearce, J.A.; Harris, N.B.W.; Tindle, A.G. 1984. Trace element discrimination diagrams for the tectonic interpretation of granitic rocks. *Journal of Petrology* **25**(4), 956–983.
- Petri, S.; Coimbra, A.M.; Amaral, G.; Ojeda y Ojeda, H.A.; Fulfaro, V.J. Ponçano, W.L. 1986. Código Brasileiro de Nomenclatura Estratigráfica — Guia de Nomenclatura Estratigráfica. *Revista Brasileira de Geociências* **16** (4), 370–415.
- Sheraton J.W. and Black, L.P. 1988. Chemical evolution of granitic rocks in the East Antarctic Shield, with particular reference to post-orogenic granites. *Lithos* **21**, 37–52.
- Souza, Z.S. 1994. *Geologia e petrogênese do "greenstone-belt Identidade: implicações sobre a evolução geodinâmica do terreno granito-"greenstone" de Rio Maria, SE do Pará.* Unpublished thesis, Universidade Federal do Pará, 472 p.
- Streckeisen, A.L. 1976. To each plutonic rock its proper name. *Earth-Science Reviews* **12**, 1–33.
- Sylvester, P.J. 1989. Post-Collisional alkaline granites. *Journal of Geology* **97**, 261–280.
- Sylvester, P.J. 1994. Archean granite plutons. In: *Archean Crustal Evolution* (edited by K. Condie), pp. 297–323. Amsterdam, Elsevier — Developments in Precambrian Geology 11.
- Tullis, J. 1983. Deformation of feldspars. In: *Feldspar Minerals*. (edited by P. H. Ribbe), pp. 297–323. Washington, Mineralogical Society of America — Reviews in Mineralogy 2.
- Whalen, J.B.; Currie, K.L.; Chappell, B.W. 1987. A-type granites: geochemical characteristics, discrimination and petrogenesis. *Contributions to Mineralogy and Petrology* **95**, 407–419.
- White, S.H.; Burrows, S.E.; Carreras, J.; Shaw, N.D.; Humphreys, F.J. 1980. On mylonites in ductile shear zones. *Journal of Structural Geology* **2** (1/2), 175–187.
- White, S.H. and Mawer, C.K. 1986. Extreme ductility from a mylonite, Parry Sound, Canada. *Journal of Structural Geology* **8** (2), 133–143.
- Wirth, K.R.; Gibbs, A.K.; Olszewski Jr, W.J. 1986. U-Pb ages of zircons from Grão-Pará group and Serra dos Carajás granite, Pará, Brazil. *Revista Brasileira de Geociências* **16** (2), 195–200.